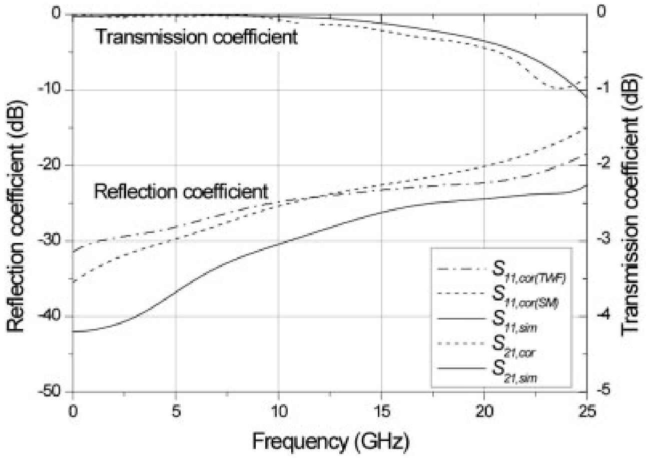

Figure 10 Reflection and transmission coefficients of the optimized SMA transition corrected for the effect of the SMA connector and the microstrip line loss

trip transition proposed in this article is better than that of the transition described in Ref. 8, where only the offset of the ground aperture has been employed in the optimization of the transition structure. Straight or right-angle coaxial-to-microstrip transitions that have been presented in the literature generally show a reflection coefficient of -15 to -10 dB at the upper edge of the operating frequency, which indicates that the transition proposed in this article offers a substantial improvement over existing transition designs. The right-angle transition can be accurately placed using the via-hole and the connector flange with respect to the microstrip line so that an excellent repeatability can be obtained by paying proper attentions to mechanical constructions.

4. CONCLUSIONS

A new method for optimizing a right-angle coaxial-to-microstrip transition has been proposed, where ground aperture and probe diameters, the offset of the ground aperture, and the microstrip stub length are simultaneously optimized to obtain the lowest signal reflection and the highest signal transmission over the entire operating frequency of the transition. Specifically, right-angle transitions between an SMA connector and a 50-Ω microstrip line on 10, 20, and 31-mil thick PTFE substrates have been designed for operation up to 20 GHz.

Measurements have been carried out for a transition on a 31-mil thick substrate, where the effect of the nonideal SMA connector used in the measurements is corrected either by calibrating out the frequency-domain characteristics of the SMA connector or by removing reflections because of the SMA connector in the time domain. Good agreements have been observed between measured and simulated characteristics of the designed transition. Measurements of the fabricated SMA transition show a reflection coefficient of less than -20 dB and a transmission coefficient of greater than -0.5 dB over 0.05–20 GHz, which indicates a substantial improvement over existing transition designs. The approach proposed in this article can be employed for the optimum design of right-angle coaxial-to-microstrip transitions widely used in printed antenna and microstrip-based circuit applications.

ACKNOWLEDGMENT

This work was supported by the Regional Research Centers Program of the Ministry of Education and Human Resources Development in Korea.

REFERENCES

1. E.H. England, A coaxial to microstrip transition, IEEE Trans Microwave Theory Tech MTT-24 (1976), 47–48.
2. R.L. Eisenhart, A better microstrip connector, IEEE MTT-S Dig 78 (1978), 318–320.
3. R. Neidert, Waveguide-to-coax-to-microstrip transitions for millimeter-wave monolithic circuits, Microwave J 26 (1983), 93–101.
4. J. Chenkin, DC to 40 GHz coaxial-to-microstrip transition for 100 GHz thick GaAs substrates, IEEE Trans Microwave Theory Tech MTT-37 (1989), 1147–1150.
5. H. Liang, J. Laskar, H.Barnes, and D. Estreich, Design and optimization for coaxial-to-microstrip transition on multilayer substrates, IEEE MTT-S Dig 3 (2001), 1915–1918.
6. W.-H. Hsu, G.-Y. Lee, and K.-L. Wong, A wideband capacitively fed circular-E patch antenna, Microwave Opt Technol Lett 27 (2000), 134–135.
7. G. Yang, M. Ali, and R. Dougal, A wideband circular polarized microstrip patch antenna for 5–6 GHz wireless LAN applications, Microwave Opt Technol Lett 45 (2005), 279–285.
8. M. Morgan and S. Weinreb, A millimeter-wave perpendicular Coax-to-microstrip transition, IEEE MTT-S Digest 2 (2002), 817–820.
9. S.A. Wartenberg and Q.H. Liu, A coaxial-to-microstrip transition for multilayer substrates, IEEE Trans Microwave Theory Tech MTT-52 (2004), 584–588.
10. D.M. Pozar, Microwave engineering, Wiley, New York, 1998, pp. 160–167, 196–205.

A DIRECTIVE PATCH ANTENNA WITH METAMATERIAL STRUCTURE

Zi-bin Weng, Nai-biao Wang, Yong-chang Jiao, and Fu-shun Zhang
National Laboratory of Antenna and Microwave Technology, Xidian University, Xi'an, Shaanxi, 710071, China

Received 8 July 2006

ABSTRACT: *A new method to improve the gain of patch antenna with metamaterial composed of ring aperture lattice is presented. The influences of the number of metamaterial layers and a comparison of electromagnetic characteristics between the conventional patch antenna and the new metamaterial patch antenna are studied by using numerical simulation method. Then, a patch antenna with the metamaterial is fabricated and measured. The simulation and experimental results show that this method is effective and this structure can realize congregating the radiation energy, thus the gain of the antenna with metamaterial can greatly increase when compared with the conventional one.* © 2006 Wiley Periodicals, Inc. Microwave Opt Technol Lett 49: 456–459, 2007; Published online in Wiley InterScience (www.interscience.wiley.com). DOI 10.1002/mop.22146

Key words: *metamaterial; directive; high gain*

1. INTRODUCTION

Metamaterials, which exhibit unique properties not existing for natural materials have attracted great interest in the last years [1–3]. Metamaterials are also called left-handed materials (LHM) in particular, in which the vectors E, H, and k form a left-handed system. Since the idea proposed by Victor Veselago in 1968 [4], the availability of such a material is taken up nowadays and extended.

In this paper, we present a new design of a high gain patch antenna using metamaterial structure. The properties of metamaterial structure and the radiation characteristics of the antennas are measured. Our studies demonstrate that the metamaterial structure can realize an effective refraction index, which approximates zero and congregate the radiation energy. Moreover, a great improvement of gain can be obtained by using the metamaterial structure on the antenna in comparison with the conventional one (Fig. 1).

2. PRINCIPLE CHARACTERISTICS OF METAMATERIAL STRUCTURE

The metamaterial is composed of copper grids with lattices whose period is equal to a (in the x-axis and y-axis directions), and the radius of the ring aperture of the copper grids is r. When the period of the square lattices is less than microwave wavelength, this structure can be seen as a metal thin-wire array [5]. This metamaterial structure has a characteristic response to electromagnetic radiation due to the plasma resonance of the electron gas. Theoretical and experimental researches have shown that such arrays of continuous thin wires are characterized by a plasma frequency [6]. Both the approximate analytical theory and rigorous homogenization theory show that the equivalent permittivity has a behavior governed by a plasma frequency in the microwave domain:

$$\varepsilon_{\text{eff}} = 1 - \omega_p^2/\omega^2 \tag{1}$$

where ω_p is the plasma frequency and ω is the frequency of the electromagnetic wave. The equivalent permittivity is negative when the frequency is below ω_p, which has been widely discussed and applied in microwave domain [7]. But the permittivity can be positive and less than one when microwave frequency is just above the plasma frequency. Thus, the permittivity can be less than one, eventually approximately zero. That is, to say, the optical index is less than one, even very close to zero. Then, a very low optical index is a very good candidate to design convergent microlenses [5].

3. SIMULATION AND NUMERICAL RESULTS

3.1 The Patch Antenna With and Without Metamaterial Cover

On the basis of the general antenna design process, the structure of the patch antenna is shown in Figure 2. The patch antenna whose driven element is coaxial probe has been designed to work at 2.57 GHz. The size of the patch antenna is 41 mm × 33.6 mm, the dielectric constant of the substrate is $\varepsilon_r = 2.65$, the thickness of the substrate is 1 mm, and the ground is 315 mm × 315 mm. The metamaterial structure is composed of very thin copper grids with square lattices whose period a is equal to 35 mm, and the radius of ring aperture in the copper grids r is 17.2 mm. The spacing between two layers in the z-axis direction is 41 mm and each layer is composed of 9 × 9 cells, the total length of edge is 315 mm. The metamaterial structure is located at 41 mm from the ground.

The properties of the metamaterial structure and the radiation characteristics of the antenna are investigated by numerical method. The simulation results are given using Ansoft HFSS 3-D simulator, which is based on the finite element method (FEM). The radiation patterns of conventional patch antenna and metamaterial

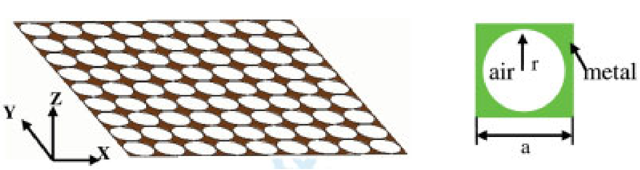

Figure 1 Schematic of proposed metamaterial. [Color figure can be viewed in the online issue, which is available at www.interscience.wiley.com]

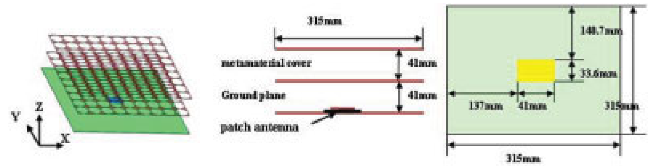

Figure 2 Patch antenna with metamaterial structure. [Color figure can be viewed in the online issue, which is available at www.interscience.wiley.com]

patch antenna are shown in Figure 3. The working frequency is 2.55 GHz. The gain of the antenna with metamaterial structure increases from the original 7.4 to 17.4 dB, which is improved observably.

3.2 The Patch Antenna With Different Number of Layers

As the foundation of the antenna design, it is necessary to analyze the effect of the number of layers. The spacing between each two layers in the z-axis direction is 41 mm. The 3-D radiation patterns of different number of layers are shown in Figure 4 in decibel scale. The results show that the beam width of the main lobe becomes narrower with the increasing number of layers. When only one layer is used to form the metamaterial cover, the convergent characteristic of this structure is not effective enough, and when the layers are added to three, the reflection of the metamaterial and the wave leakage are enhanced, as a result, the gain of this antenna with three layers is not high enough. The size of the cover and the ground could be enlarged to improve the wave leakage, but the dimension will become too large for its practical use. We can conclude that only when the metamaterial cover is made up of two layers can get an optimum gain.

4. EXPERIMENT AND RESULTS

To validate our design, a patch antenna with metamaterial is fabricated and measured. The structure is shown in Figure 5.

The measured VSWR of the metamaterial patch antenna and the conventional patch antenna are shown in Figure 6. The figure indicates that the working frequency of the patch antenna shifts slightly to 2.53 GHz in the presence of the metamaterial cover. So, the working frequency is selected at 2.55 GHz for both the conventional and the metamaterial one. The patterns of the patch antenna with and without metamaterial cover have been measured in far field chamber at a distance of about 6 m (in order to be in a far field configuration). The transmitting antenna is a ridged horn BJ22, a pyramidal horn is used as a standard antenna for measuring the gain of the patch antenna, and a network analyzer is used for the measurements. The patterns of the system have been measured

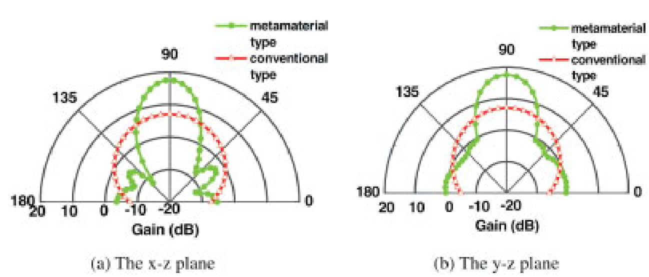

Figure 3 Radiation patterns of the conventional patch antenna and the metamaterial patch antenna. (a) The x–z plane. (b) The y–z plane. (a) The x–z plane (b) The y–z plane. [Color figure can be viewed in the online issue, which is available at www.interscience.wiley.com]

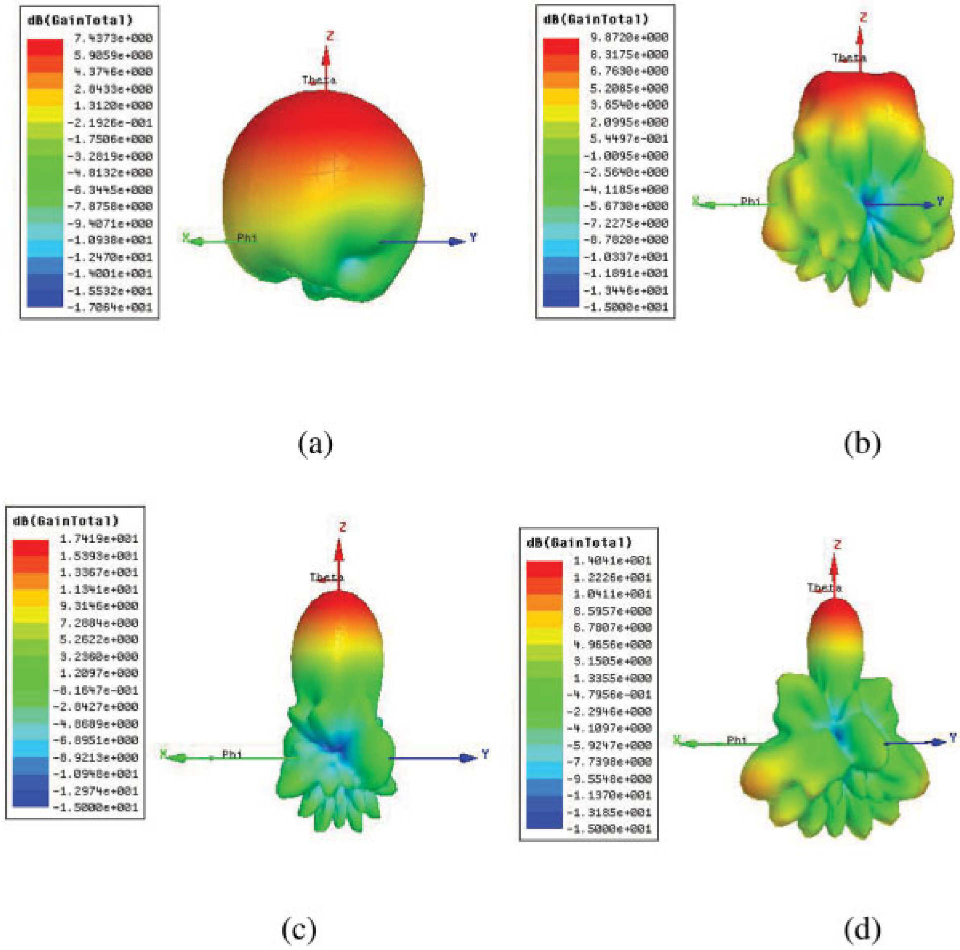

Figure 4 Three-dimensional radiation patterns of patch antenna with different number of metamaterial layers. (a) Without cover. (b) One layer. (c) Two layers. (d) Three layers. [Color figure can be viewed in the online issue, which is available at www.interscience.wiley.com]

in two orthogonal planes: one is the x–z plane and the other is the y–z plane. Figure 7 shows the measured radiation patterns for the conventional patch antenna and the metamaterial patch antenna in the x–z plane and the y–z plane. Some electrical characteristics of the antenna are shown in Table 1. The effect of the spacing between two layers of metamaterial structure is also studied. The curve of the gain, which is changed with the spacing between two layers, is shown in Figure 8. Good agreements between the predicted and measured results are observed from these figures. The measured results validate that it is effectual to raise the gain of the patch antenna by using metamaterial structure.

In theory, the maximum directivity of this antenna is Dmax $= 4\pi A/\lambda02$, *where* $A = 315$ mm $\times$ 315 mm, $\lambda_0 = c_0/f_0 = 117.6$ mm, and the gain $G_{\max} = kD_{\max}$, k is the efficiency. It is assumed $k = 1$, then it is approximate to take $G_{\max}(dB) = 10\log(4\pi A/\lambda_0^2)$, so the

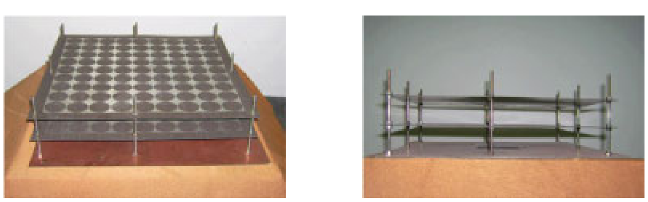

Figure 5 Photograph of the patch antenna with metamaterial. [Color figure can be viewed in the online issue, which is available at www.interscience.wiley.com]

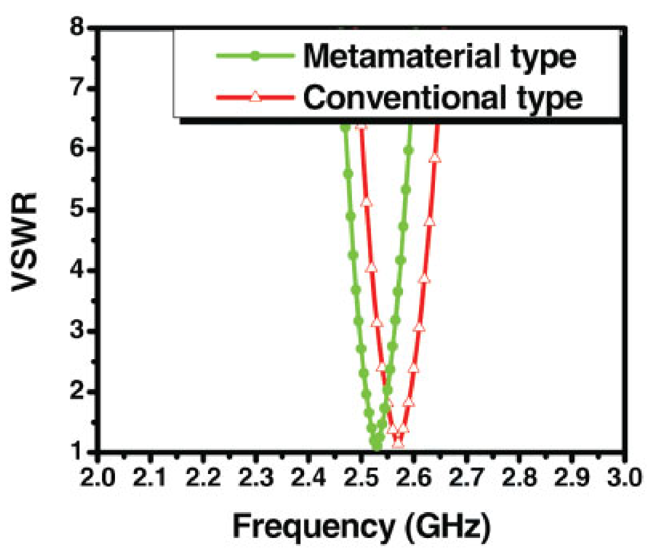

Figure 6 Measured VSWR of the conventional patch antenna and the metamaterial patch antenna. [Color figure can be viewed in the online issue, which is available at www.interscience.wiley.com]

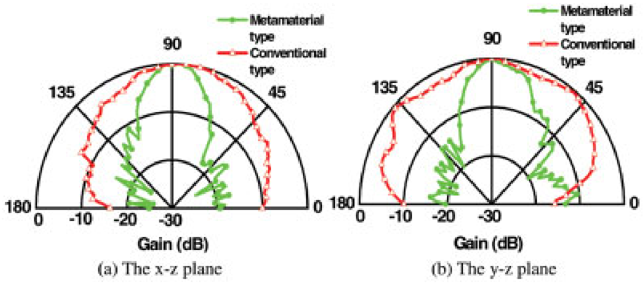

Figure 7 Measured radiation patterns for the conventional patch antenna and the metamaterial patch antenna. (a) The *x*–*z* plane. (b) The *y*–*z* plane. (a) The *x*–*z* plane (b) The *y*–*z* plane. [Color figure can be viewed in the online issue, which is available at www.interscience.wiley.com]

theoretical maximum value of the antenna gain is 19.5 dB. The gain of the patch antenna with metamaterial structure is already very close to the theoretical maximum value of antenna with the same size and operating frequency.

5. CONCLUSION

A new patch antenna with a metamaterial cover has been designed. Then, the radiation characteristics of a patch antenna with and without metamaterial structure are measured. The measured results show an about 10 dB addition in the antenna gain in comparison with the conventional antenna, thus the radiation characteristics of antenna with metamaterial structure are remarkably improved. Since, the ring aperture lattice is insensitive to the direction of arrival wave and independent to the wave polarization, this structure is much more useful than some kinds of EBG covers in some specific applications.

TABLE 1 The Electrical Characteristics of the Patch Antenna With and Without Cover

	Frequency (GHz)	Gain (dB)	HPBW ($x-z$-Plane)	HPBW ($y-z$-Plane)
Conventional type	2.55	6.8	63°	117°
Metamaterial type	2.55	17.2	25°	27°

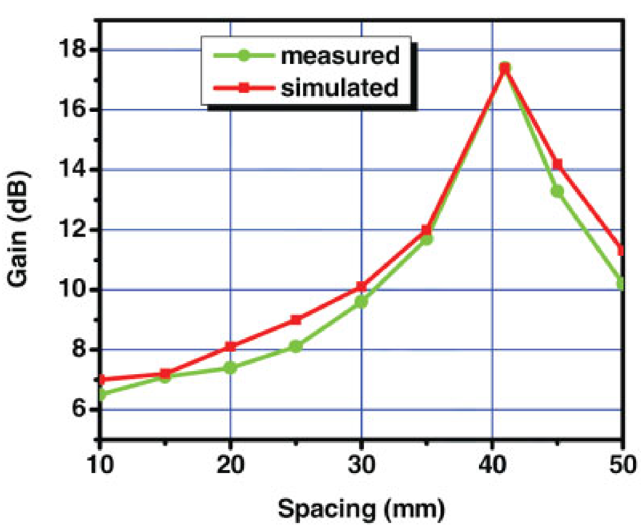

Figure 8 Gain of antenna with different spacing between two layers. [Color figure can be viewed in the online issue, which is available at www.interscience.wiley.com]

REFERENCES

1. D.R. Smith, W.J. Padilla, D.C. Vier, et al, Composite medium with simultaneously negative permeability and permittivity, Phys Rev Lett 84 (2000), 4184–4187.
2. J.B. Pendry, Negative refraction males a prefect lens, Phys Rev Lett, 85 (2000), 3966–3969.
3. L.V. Lindell, S.A. Tretyakov, K.I. Nikoskinen, and S. Ilvonen, BW media—Media with negative paraments, capable of supporting backward waves, Microwave Opt Tech Lett 31 (2001), 129–133.
4. V.G. Veselago, The electrodynamics of substances with simultaneously negative values of ε and μ, Soviet Phys USPEKI 10 (1968), 509–514.
5. S. Enoch, G. Tayeb, P. Sabouroux, and P. Vincont, A metamaterial for directive emission, Phys Rev Lett 89 (2002), 213902.
6. J. B. Pendry, A.J. Holden, W. J. Stewart, et al., Extremely low frequency plasmons in metallic mesostructures. Phys Rev Lett 76 (1996), 4773–4776.
7. M. The‘venot, C. Cheype, A. Reineix, and B. Jecko, Directive photonic band-gap antennas, IEEE Trans Microwave Theory Tech 47 (1999), 2115.

ULTRAWIDEBAND MONOCYCLE PULSE GENERATOR WITH DUAL RESISTIVE LOADED SHUNT STUBS

Tzyh-Ghuang Ma, Chin-Jay Wu, Po-Kai Cheng, and Chin-Feng Chou
Department of Electrical Engineering, National Taiwan University of Science and Technology, Taipei, Taiwan 10607, Republic of China

Received 9 July 2006

ABSTRACT: *An ultrawideband (UWB) monocycle pulse generator with dual resistive loaded shunt stubs is present in this article. The proposed pulse generator consists of a step recovery diode (SRD), a Schottky diode, a pair of resistive loaded stubs, and a pair of short-circuited stubs. By introducing an additional resistive loaded stub between the SRD and the Schottky diode, the ringing tail of the impulse waveform can be substantially suppressed and the resultant monocycle pulse is well-behaved with very low ringing level. The measurement result demonstrates a monocycle pulse with peak-to-peak amplitude of 550 mV, pulsewidth of 320 ps, ringing level of as low as −22 dB, and good pulse symmetry. This pulse generator is suitable for various UWB applications.* © 2006 Wiley Periodicals, Inc. Microwave Opt Technol Lett 49: 459–462, 2007; Published online in Wiley InterScience (www.interscience.wiley.com). DOI 10.1002/mop.22145

Key words: *pulse generator; ultrawideband radio; Gaussian impulse; monocycle pulse*

1. INTRODUCTION

Ultrawideband (UWB) technology has received more and more attention in recent years because of the increased demands on wireless personal area networks (WPANs) [1] as well as on high-resolution positioning facilities such as wireless sensor networks (WSNs) [2]. The basic idea behind this promising technology is transmitting and receiving subnanosecond pulses directly without implementing conventional up-/down-conversion circuit topologies. Ultrashort pulses with well-defined shapes therefore play a crucial role in the UWB transceiver design. In the transmitter, Gaussian or monocycle pulses are generated by a pulse generator and transmitted to free space via UWB antenna. In the receiver, on the other hand, received pulses are sampled by a microwave sampler and correlated with template pulses for data detection. The